# Additive scaling law for structural organization of chromatin in chicken erythrocyte nuclei

E. G. Iashina,[1,2] E. V. Velichko,[3] M. V. Filatov,[1] W. G. Bouwman,[3] C. P. Duif,[3] A. Brulet,[4] and S. V. Grigoriev[1,2]

[1]*Petersburg Nuclear Physics Institute, Gatchina, St. Petersburg 188300, Russia*

[2]*Saint Petersburg State University, Ulyanovskaya 1, St. Petersburg 198504, Russia*

[3]*Delft University of Technology, Mekelweg 15, 2629 JB Delft, Netherlands*

[4]*Leon Brillouin Laboratory, CEA Saclay, 91191 Gif sur Yvette Cedex, France*

(Received 19 January 2017; published 19 July 2017)

Small-angle neutron scattering (SANS) on nuclei of chicken erythrocytes demonstrates the cubic dependence of the scattering intensity $Q^{-3}$ in the range of momentum transfer $Q \in 10^{-3}$–$10^{-2}$ nm$^{-1}$. Independent spin-echo SANS measurements give the spin-echo function, which is well described by the exponential law in a range of sizes $(3 \times 10^2)$–$(3 \times 10^4)$ nm. Both experimental dependences reflect the nature of the structural organization of chromatin in the nucleus of a living cell, which corresponds to the correlation function $\gamma(r) = \ln(\xi/r)$ for $r < \xi$, where $\xi = (3.69 \pm 0.07) \times 10^3$ nm, the size of the nucleus. It has the specific scaling property of the logarithmic fractal $\gamma(r/a) = \gamma(r) + \ln(a)$, i.e., the scaling down by $a$ gives an additive constant to the correlation function, which distinguishes it from the mass fractal, which is characterized by multiplicative constant.

DOI: 10.1103/PhysRevE.96.012411

## I. INTRODUCTION

The structural and functional design of organisms was formed under the influence of two important factors. The first of them is the tendency to maximize the metabolic capacity, because it produces energy and substances necessary for the maintenance and reproduction of life. It is achieved by increasing the surface area through which there is the interchange of resources with the environment. The second factor is the increase of the internal efficiency by means of decreasing the distance of material transportation and therefore the time necessary for transportation [1]. This tendency leads to the compaction of the living system or, in other words, to the minimization of an object. These two tendencies are in opposition to each other and the morphology of a living organism evolving under the influence of two antagonistic factors takes the shape that is considered as the most favorable for survival.

Furthermore, the simplicity of the laws of reproduction is the third yet not the least important property, which is pursued by the life forms. In nature the structures are often generated by multiple repetition of the same morphogenetic mechanism, for example, the branching. A tree is the most illustrative example of the realization of this mechanism. It grows in a way that on each successive level of branching, the sum of squares of radii of the branches equals the square of the radius of the branch that was divided. The property of recurrence describing the growth of a tree was first noted long ago by da Vinci [2].

Although recent decades have seen impressive achievements in biology and genetics, the determination of the structural organization of chromatin in the nucleus *in vivo* remains one of the main unresolved questions. Chromatin is a complex consisting of DNA molecules and proteins, which are in charge of the storage of genetic information. A DNA molecule is a left-handed double helix. Knowing how certain genes within DNA operate, we still do not know the general principles of chromatin packaging in the nucleus. It is apparent that it is the structural organization of chromatin that results in the highest degree of its compactness. However, the question of how a meter-long DNA strand is packed into a micron nucleus is not completely resolved. The general principles of transportation of low-molecular compounds and macromolecular complexes in a cell nucleus are even less understood. The principles of transportation are supposed to be directly connected with and are likely to be determined by the particularities of a structural packaging of chromatin. Such a structure should facilitate the rapid transportation.

The DNA packaging in chromatin on a nanometer length scale is provided by nucleosomes. The structure of a nucleosome consists of a disk-shaped histone core around which the DNA is tightly wrapped in a left-handed coil of 1.7 turns [3]. The existence of discrete repeating units in chromatin was discovered with the help of the electron microscope. The chromatin was reported to resemble the bead-on-a-string structure [4,5]. Each "bead" contains the DNA segment with a length of 150–200 pairs of nucleotides and eight molecules of histones of different types [6]. A separate nucleosome consists of a protein core on which the DNA molecule is wound. The DNA molecule performs 1.67 rotations around the nucleosome core. Nucleosomes make the DNA molecule approximately 7 times shorter. They were discovered in all eukaryotic cells and even in DNA-containing viruses. The ways of nucleosome packaging into the solid chromatin thread have been discussed since the time when the first images of scanning electron microscopy were attained [7–14]. Several models were suggested for this matter. In the solenoid model the chain of nucleosomes is twisted into a superhelix, one coil of which has six nucleosomes, while the helix pitch distance is 11 nm. In a zigzag model the incoming and outgoing DNA strands form a contact resulting in a dense spiral packing characterized by a larger distance between the neighboring nucleosomes in a chain as compared to the distance between the nucleosomes separated by one or more nucleosomes.

The DNA molecules are 2 nm in diameter and their length can reach up to several meters (human DNA is about 1.8 m in length). The largest genome size is nowadays attributed to Amoeba dubia, conveniently 200 times larger than a human's [15]. It is obvious that the packaging of such long molecules into a cell nucleus only 2–10 $\mu$m in diameter must be extremely regular. The problem of packaging of DNA molecules into a limited nucleus volume is complicated by the

 

fact that it is at the same time necessary to open the possibility of localized DNA unpacking and the provision of an access of ferments of replication and transcription. That is why the chromatin in a cell nucleus forms complex spatial structures with several levels of organization.

The large-scale organization of chromatin is fundamentally different from its small-scale structure [16–21]. At present the most popular model describing the three-dimensional configuration of chromatin packaging in a cell nucleus is represented by a crumpled or fractal globule. It was shown in [22,23] that the packing of DNA in a chromosome has the structure of a crumpled globule. The crumpled globule is an open macromolecule with hierarchically self-similar packing of the polymer chain. Packing the chain in a crumpled globule is similar to the trajectory of an ultrametric random walk [24,25].

The model of a crumpled globule explains how a rather long piece of DNA can be reversibly and quickly folded and unpacked when reading the genetic information. The model suggests that the chromatin fiber is packed in a self-similar manner resembling the Peano (space-filling) curve, well known in the theory of fractals [26], which has three dimensions and fills the three-dimensional space completely.

Recently, Tamm *et al.* [27] showed a computer simulation of the dynamics of the thermal motion of monomers forming a crumpled globule. It was proved that the crumpled globule self-diffusion is much faster than in the equilibrium tangled globule, the so-called Gaussian tangle.

Experiments on small-angle neutron scattering (SANS) have shown a bifractal structure of the DNA molecule, confirming the fundamental difference between small-scale and large-scale structures of the DNA package [18,19]. It was found that the exponent $D$ of the power function $I(Q) \sim Q^{-D}$ in the cross section of small-angle neutron scattering equals 2.4 on the scale of 20–400 nm and it is close to 3 on the scale from 400 nm to 1500 $\mu$m [18]. In the framework of the fractal concept $D = 2.4$ corresponds to the volume (mass) fractal with the fractal dimension $D_m = 2.4$.

The exponent close to 3 was until recently interpreted as not of any particular interest on its own, being the intermediate case of the transition from mass to surface fractal. As shown below, the cubic dependence on the cross section of small-angle neutron scattering corresponds to a very special type of fractal organization of matter, the logarithmic fractal.

Here we present the results of studies of the structural organization of chromatin obtained by two different techniques of small-angle neutron scattering (SANS and spin-echo SANS). The results show that the correlation function describing the large-scale structure of the chromatin organization in the cell nucleus represents a logarithmic dependence $\gamma(r) \sim \ln(\xi/r)$, i.e., the structure of chromatin forms a logarithmic fractal, which is fundamentally different from the mass or surface fractals.

## II. SMALL-ANGLE NEUTRON SCATTERING FROM INTERPHASE CHICKEN ERYTHROCYTE NUCLEI

Small-angle neutron scattering is one of the most informative techniques for studying the structure of matter at supra-atomic scales from a few nanometers to a few microns. The intensity of neutron scattering $I(Q)$ measured in the experiment is directly related to the pair correlation function of the object $\gamma(r)$, where there was a scattering

$$\gamma(r) = \frac{1}{2\pi} \int_0^\infty I(Q) \frac{\sin(Qr)}{Qr} r^2 dr. \quad (1)$$

The study of the small-scale structure of the chromatin in the isolated chicken erythrocyte nuclei was carried out on a PA20 instrument (LLB, Saclay, France) in the momentum transfer range $10^{-2}$–$10^{0}$ nm$^{-1}$. The large-scale chromatin structure was studied on an ultrasmall-angle neutron scattering instrument TPA (LLB, Saclay, France) in the momentum transfer range $10^{-3}$–$10^{-2}$ nm$^{-1}$. The same sample was used to perform both experiments. Chicken erythrocytes were obtained by repeated washing in an isotonic phosphate buffer, $p$H 7.4, containing 10 mM ethylenediamine tetra-acetic acid (EDTA) and centrifugation to remove plasma proteins. The outer cytoplasmic membrane was solubilized by the nonionic detergent Triton X-100 (a 0.2% solution in a phosphate buffer, $p$H 7.4). The isolated cell nuclei were fixed with a 0.05% glutaraldehyde solution for 10 min. Then the fixing agent was removed by centrifugation. The cell nuclei were stored in a phosphate buffer, $p$H 7.4, containing 20 mM EDTA to prevent the DNA degradation by nucleases. In order to achieve the maximum contrast, the nuclei of the cells were placed in buffer containing $D_2O$ with a concentration of more than 95%. In addition to maximally increasing the neutron scattering intensity, we used the densest solution possible for these samples.

The combined results of both experiments are shown in Fig. 1. The intensity of small-angle neutron scattering in the momentum transfer range $10^{-2}$–$10^{-1}$ nm$^{-1}$ is described by a power function $I(Q) \sim Q^{-D}$ with the power $D = 2.46 \pm 0.01$. This dependence demonstrates the fractal organization of

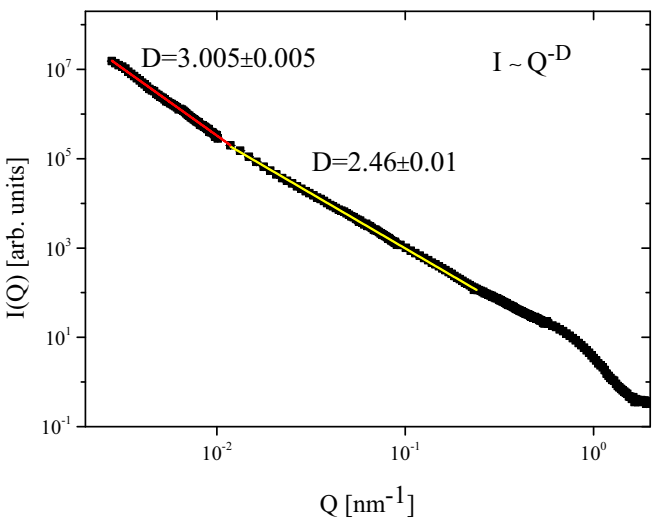


FIG. 1. Small-angle neutron scattering on nuclei of chicken erythrocytes. The data for the intensity of neutron scattering in the momentum transfer range $10^{-3}$–$10^{-2}$ nm$^{-1}$ were obtained from the TPA instrument at LLB, Saclay, France. The data for the intensity of neutron scattering in the momentum transfer range $10^{-2}$–$10^{0}$ nm$^{-1}$ were obtained from the PA20 instrument at LLB, Saclay, France.

DNA packaging in the nucleus with the dimension equal to the power $D$. The intensity of neutron scattering in the momentum transfer range $10^{-3}$–$10^{-2}$ nm$^{-1}$ also has a power dependence with the power $D = 3.005 \pm 0.005$. The difference between the indices observed in different ranges of the momentum transfer $Q$ leads to the conclusion that the fractal structure of the DNA in the nucleus changes its nature at the transition from small scale (tens of nanometers) to larger scale (hundreds of nanometers). Thus, the results presented in Fig. 1 confirm the conclusions of Refs. [18,19], showing that the nuclei of chicken erythrocytes have a bifractal structure of the DNA molecule.

The correlation function of the object, characterized by the law of the scattering of $Q^{-D}$ with $2 < D < 3$, corresponds to a mass fractal with dimension $D$ and is described by the expression $\gamma(r) \sim (r/\xi)^{D-3}$. With $D$ approaching 3, the correlation function changes its nature and can be described by the ratio $\gamma(r) \sim \ln(\xi/r)$. The changing of the nature of the correlation function leads to a fundamental change of properties and structure of the DNA packaging in the cell nucleus.

## III. SPIN-ECHO SMALL-ANGLE NEUTRON SCATTERING FROM INTERPHASE CHICKEN ERYTHROCYTE NUCLEI

To confirm the unusual fractal properties of DNA packaging in the nucleus on a large scale of the order of 1 $\mu$m, the technique of spin-echo small-angle neutron scattering (SESANS) was used, which allows the study of inhomogeneities on scales from 20 nm up to 20 $\mu$m [28–33]. This method gives reliable information on the correlation length of the object, which sometimes cannot be determined with the help of conventional SANS technique because of the resolution limitations.

The experiments are carried out on a SESANS instrument of the Delft University of Technology on the same sample in heavy water with a concentration of more than 95%. In the spin-echo SANS technique the phenomenon of Larmor precession of the neutron magnetic moment in a magnetic field is employed to decode the scattering angle in the interaction of neutrons with the particle [28]. In the experiment the polarization of the neutron beam is measured as it passes through the sample. We perform the scan along the spatial coordinate $z$, which is perpendicular to the direction of the neutron beam, called the spin-echo length.

The measured polarization of $P(z)$ depends on the properties of the sample and is described as follows [29]:

$$P(z) = \exp\{l\sigma[G(z) - 1]\}, \tag{2}$$

where $l$ is the thickness of the sample, $\sigma$ is total cross section of neutron scattering on the sample, and $G(z)$ is the SESANS correlation function for the object. For isotropic systems, the function $G(z)$ is connected with the spatial correlation function $\gamma(r)$ by the Abel transformation [30]

$$\gamma(r) = -\frac{\xi}{\pi}\int_r^\infty \frac{G'(z)}{\sqrt{z^2 - r^2}}dz. \tag{3}$$

Thus, the measurement and description of the function $G(z)$ clearly provide a description of the function $\gamma(r)$ without any loss of information.

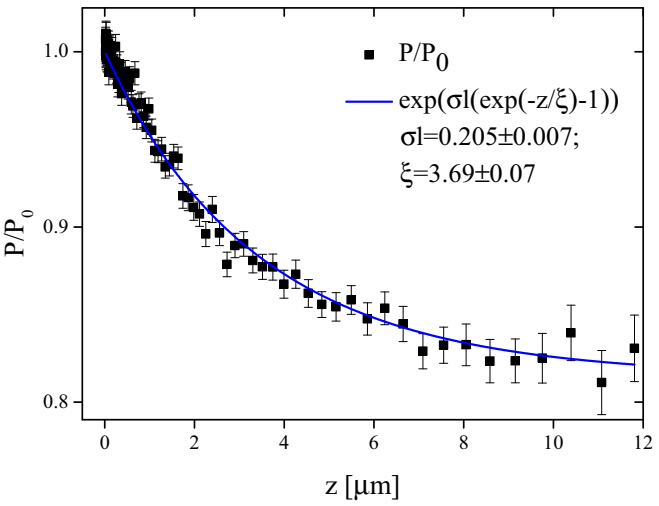


FIG. 2. Normalized SESANS polarization $P/P_0$ as a function of $z$ on chicken erythrocyte nuclei. The line represents fit $\exp(\sigma l(\exp(-z/\xi) - 1))$, with $\sigma l = 0.205 \pm 0.007$ and $\xi = (3.69 \pm 0.07) \times 10^3$ nm.

Figure 2 shows the results of the measurement of the polarization $P/P_0$ as a function of the spin-echo (SE) length $z$ on chicken erythrocytes nuclei. Experimental data demonstrate clearly the exponential law for the SESANS function (Fig. 3)

$$G(z) = \exp(-z/\xi), \tag{4}$$

where $\xi = (3.69 \pm 0.07) \times 10^3$ nm is the correlation length of the sample, which is the size of the nucleus. It is worth noting that the SESANS technique is an integral method and contains information about the structure on all scales simultaneously; however, the main contribution is made by the structure of the micron scale.

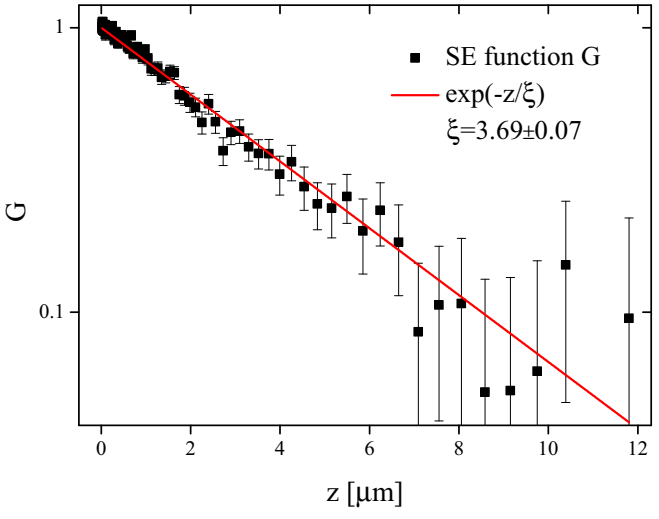


FIG. 3. The log-lin plot of the SESANS function from isolated chicken erythrocyte nuclei. The data demonstrate the exponential law for the one-dimensional correlation function $G(z) = \exp(-z/\xi)$, with $\xi = (3.69 \pm 0.07) \times 10^3$ nm.

## IV. LARGE-SCALE CHROMATIN ORGANIZATION IN INTERPHASE NUCLEI

The SESANS method is a method complementary to the SANS technique, since in both methods the spatial correlation function of the scattering object is measured [33]. The Hankel transform relates the SE function $G(z)$ and scattering cross section $I(Q)$ to each other for isotropic scattering [30]

$$G(z) = \frac{2\pi}{k_0^2 \sigma \xi^2} \int_0^\infty J_0(zQ) I(Q) Q \, dQ. \tag{5}$$

Using the Fourier transform (1) and Hankel transform (5) it is easy to show that the momentum transfer dependence of the SANS intensity

$$I(Q) = A[1 + (Q\xi)^2]^{-3/2} \tag{6}$$

and the spin-echo length dependence of the SESANS function

$$G(z) = \exp(-z/\xi) \tag{7}$$

correspond to the spatial correlation function of the form

$$\gamma(r) = \frac{1}{\pi} K_0(r/\xi), \tag{8}$$

where $K_0(x)$ is a zeroth-order modified Bessel function of the second kind [34]. In the region of small $r$ ($r/\xi < 1$), or inside the particle, the function (8) has a logarithmic nature

$$K_0(r/\xi) \simeq \ln(\xi/r). \tag{9}$$

Such behavior of the correlation function corresponds to a special type of fractal object, which is different from the mass and surface fractals. It is easily observed that the correlation function (9) has the scaling property

$$\gamma(r/a) = \gamma(r) + \ln(a), \tag{10}$$

i.e., scaling down gives an additive constant to the correlation function, and not the multiplicative one, as in the case of mass fractal.

By definition, the spatial correlation function is the probability of finding a nonzero density on different scales. Knowledge of the correlation function allows one to find the volume occupied by the particle. Integrating $\gamma(r)$ in three-dimensional space, we obtain

$$V(r) = 4\pi \int_0^r r'^2 \gamma(r') dr'. \tag{11}$$

In our case of the logarithmic fractal, the integral (10) equals

$$V(r) \sim r^3 \ln(\xi/r). \tag{12}$$

It ought to be noted that the volume is a special case of the notion of the mathematical measure. The Hausdorff measure, or the $D_f$ measure, is introduced [35] to describe fractal sets

$$\mu_{D_f}(r) = r^{D_f}, \tag{13}$$

where $D_f$ is a Hausdorff-Besicovitch dimension, which takes fractional values. The number of spheres of $r$ size needed to fill in the regular fractal equals

$$N(r) = r^{-D_f}. \tag{14}$$

A fractal is defined as a set whose Hausdorff-Besicovitch dimension $D_f$ is larger than the topological dimension $D_T$. It is determined by means of coverings, for example, for a point $D_T = 0$, the line segment $D_T = 1$, for a plane figure $D_T = 2$, etc. This definition describes the regular fractals, such as Cantor dust, the Koch snowflake, the Sierpinski sponge, and carpet and dragon curves. They all have a regular-shaped, regular structure. Each fragment of such a regular-shaped fractal repeats precisely the entire structure as a whole.

However, there are objects for which the dimension coincides with its Hausdorff dimension $D_T = D_f$, but at the same time they are neither a line segment nor a plane nor a ball. The fact is that they are described with a logarithmic measure, not a Hausdorff measure (13):

$$\mu(r) = r^{D_f} \ln^{\Delta}(1/r), \tag{15}$$

where $\Delta$ is a subdimension [35].

This is due to the fact that the Hausdorff-Besicovitch dimension is not sufficient to describe them, since such objects are characterized by a hierarchical structure that reflects the presence of the logarithm. Further, the nature of hierarchy is reflected in the value of the subdimension. A negative value of subdimension carries a constructive hierarchy. The next generation of the fractal is built on the previous generation. In the case of a positive subdimension the hierarchy is destructive and the following generation is subtracted from the previous one. In both cases, the absolute value of subdimension reflects the rate of change between generations. The analogs of destructive and constructive structure of regular fractals are the Koch snowflake and the Sierpinski carpet, respectively. In the first case the fractal is built by adding the line segments, in the second case by subtracting the triangles. The number of coverings required to tile the logarithmic fractal equals

$$N(r) = r^{-D_f} \ln^{-\Delta}(1/r). \tag{16}$$

It is important to note that many biological objects have the structure of logarithmic fractals. The law of tree growth is described by a logarithmic fractal with $D_F = 2$ and $\Delta = -1$ [36]. This model implies a change in cross section of the branches, while their length can be arbitrary. Therefore, both fractal dimension and topological dimension of this fractal equal 2. Negative subdimension means that the fractal grows with every tree branching by means of the increase in the cross section of the branches and their area and number depend on the level of branching. A fractal is constructed from the sum of all sections at each level of branching. The absolute value of subdimension equal to 1 means that on each $n$th iteration the area of the fractal increases by the same value, equal to the area of the first generation $S_n = nS_1$, so the da Vinci rule is applicable.

The bronchial branching in the lungs is described by a logarithmic fractal with $D_F = 3$ and $\Delta = -1$. It is constructed in a way similar to the previous one, but instead on two-dimensional sections the third-dimensional cylinders are used, which are characterized by volume. This structure provides the least air resistance in the lungs. In this case the following condition is fulfilled: the dependence constancy of resistance and the cross section in all parts of the system, both before and after the branching [35].

The structural organization of chromatin in the nuclei of chicken erythrocytes is a logarithmic fractal with $D_F = 3$ and $\Delta = 1$ on scales of hundreds to thousands of nanometers. Here

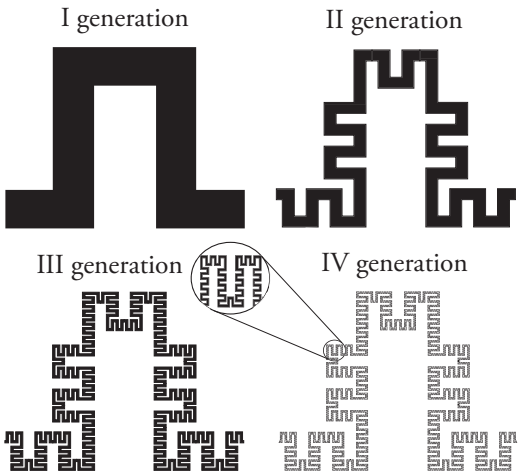


FIG. 4. Construction of the logarithmic fractal that describes the structural organization of chromatin in four generations.

we deal with the destructive hierarchy. Starting with the dense three-dimensional space, with each iteration we subtract the volume so the following condition on each iteration is fulfilled: $V_n = V_{n+1}/n$. For the sake of simplicity, we draw this fractal on a plane, where the area acts as the volume (Fig. 4). In the first iteration the area is subtracted from the dense space, forming the primary fold, so the volume is reduced by half. Further, the area is subtracted from the place where the fold is homogeneous, forming folds of the second generation, and the volume occupied by the fractal is equal to one-third of the original one. The number and density of folds on each next generation increase.

The following analogy with the tree is appropriate in the sense that every fold is a branch that originates other smaller and more numerous branch folds. The number, density, and of course the size of the folds of the branches depend on their generation.

## V. CONCLUSION

The term crumpled globule came from polymer science. There are many facts confirming that the model of the fractal globule describes large-scale chromatin packing [18,19,23,25,27,37,38]. In this paper we have shown that in terms of small-angle neutron scattering a fractal globule is a logarithmic fractal with dimension 3 and subdimension 1. Moreover, this means that spatial organization of chromatin in the nucleus of chicken erythrocytes is described by the law of the branching in the range from 500 to 3700 nm. This DNA branching permeates the entire cell. The DNA strand has a hierarchically branched structure similar to a three-dimensional spherically symmetric tree of folds, which ensures the maximum availability of any section from the outside and the most compact, dense structure. Apparently, such structure is characteristic for living systems.

## ACKNOWLEDGMENTS

The authors would like to thank D. V. Lebedev for the assistance rendered. The work was supported by the Russian Foundation for Basic Research, the Ministry of Education of the Russian Federation, through Grant No. 17-02-00313 A.

[1] G. B. West, J. H. Brown, and B. J. Enquist, Science **284**, 1677 (1999).
[2] C. Eloy, Phys. Rev. Lett. **107**, 258101 (2011).
[3] B. Alberts, *Molecular Biology of the Cell* (Garland Science, New York, 2008), Chap. 4.
[4] D. R. Hewish and L. A. Burgoyne, Biochem. Biophys. Res. Commun. **52**, 504 (1973).
[5] A. Olins and D. Olince, Science **183**, 330 (1974).
[6] R. D. Kornberg, Science **184**, 868 (1947).
[7] J. Finch and A. Klug, Proc. Natl. Acad. Sci. U.S.A. **73**, 1897 (1976).
[8] F. Thoma and T. Koller, Cell **12**, 101 (1977).
[9] C. L. Woodcock, L. L. Frado, and J. B. Rattner, J. Cell Biol. **99**, 42 (1984).
[10] J. Bednar, R. Horowitz, J. Dubochet, and C. Woodcock, J. Cell Biol. **131**, 1365 (1995).
[11] J. Bednar, R. Horowitz, S. Grigoryev, L. Carruthers, J. Hansen, A. Koster, and C. Woodcock, Proc. Natl. Acad. Sci. U.S.A. **95**, 14173 (1998).
[12] P. Robinson and D. Rhodes, Curr. Opin. Struct. Biol. **16**, 336 (2006).
[13] C. L. Woodcock and R. P. Ghosh, Cold Spring Harb. Perspect. Biol. **2**, a000596 (2010).
[14] E. Fussner, R. W. Ching, and D. P. Bazett-Jones, Trends Biochem. Sci. **36**, 1 (2011).
[15] T. R. Gregory and P. D. N. Hebert, Genome Res. **9**, 317 (1999).
[16] D. Gerlich and J. Ellenberg, Curr. Opin. Cell Biol. **15**, 664 (2003).
[17] A. Belmont, Curr. Opin. Cell Biol. **15**, 304 (2003).
[18] D. V. Lebedev, M. V. Filatov, A. I. Kuklin, A. K. Islamov, E. Kentzinger, R. Pantina, B. P. Toperverg, and V. V. Isaev-Ivanov, FEBS Lett. **579**, 1465 (2005).
[19] A. V. Ilatovskiy, D. V. Lebedev, M. V. Filatov, M. G. Petukhov, and V. V. Isaev-Ivanov, J. Phys.: Conf. Ser. **351**, 012007 (2012).
[20] K. Metze, Expert Rev. Mol. Diagn. **13**, 719 (2013).
[21] T. Misteli, Science **291**, 843 (2001).
[22] E. Lieberman-Aiden, N. L. van Berkum, L. Williams, M. Imakaev, T. Ragoczy, A. Telling, I. Amit, B. R. Lajoie, P. J. Sabo, M. O. Dorschner, R. Sandstrom, B. Bernstein, M. A. Bender, M. Groudine, A. Gnirke, J. Stamatoyannopoulos, L. A. Mirny, E. S. Lander, and J. Dekker, Science **326**, 289 (2009).
[23] L. A. Mirny, Cromosome Res. **19**, 37 (2011).
[24] A. I. Olemskoi and A. Y. Flat, Usp. Fiz. Nauk **163**, 1 (1993).
[25] V. A. Avetisov, V. A. Ivanov, D. A. Meshkov, and S. K. Nechaev, JETP Lett. **98**, 242 (2013).
[26] V. A. Avetisov, V. A. Ivanov, D. A. Meshkov, and S. K. Nechaev, Biophys. J. **107**, 2361 (2014).
[27] M. V. Tamm, L. I. Nazarov, A. A. Gavrilov, and A. V. Chertovich, Phys. Rev. Lett. **114**, 178102 (2015).

[28] M. T. Rekveldt, Nucl. Instrum. Methods Phys. Res. Sect. B **114**, 366 (1996).
[29] M. T. Rekveldt, J. Plomp, W. G. Bouwman, W. H. Kraan, S. V. Grigoriev, and M. Blaauw, Rev. Sci. Instrum. **76**, 033901 (2005).
[30] R. Andersson, L. F. van Heijkamp, I. M. de Schepper, and W. G. Bouwman, J. Appl. Crystallogr. **41**, 868 (2008).
[31] W. G. Bouwman, T. V. Krouglov, J. Plomp, and M. T. Rekveldt, Physica B **357**, 66 (2004).
[32] T. Krouglov, W. G. Bouwman, J. Plomp, M. T. Rekveldt, G. J. Vroege, A. V. Petukhov, and D. M. E. Thies-Weesie, J. Appl. Crystallogr. **36**, 1417 (2003).
[33] T. Krouglov, I. M. de Schepper, W. G. Bouwman, and M. T. Rekveldt, J. Appl. Crystallogr. **36**, 117 (2003).
[34] I. S. Gradshteyn and I. M. Ryzhik, *Table of Integrals, Series, and Products* (Fizmatlit, Moscow, 1963; Academic, New York, 1994).
[35] B. Mandelbrot, *The Fractal Geometry of Nature* (Freeman, New York, 1983).
[36] J. O. Indekeu and G. Fleerackers, Physica A **261**, 294 (1998).
[37] J. Dekker, M. A. Marti-Renom, and L. A. Mirny, Nat. Rev. Genet. **14**, 390 (2013).
[38] M. Barbieria, M. Chotaliab, J. Fraserc, L.-M. Lavitasb, J. Dostiec, A. Pombob, and M. Nicodemi, Proc. Natl. Acad. Sci. U.S.A. **109**, 16173 (2012).